A Multi-phasic Approach for Estimating the Biot Coefficient for Grimsel Granite

A.P.S. Selvadurai[a,*], Paul A. Selvadurai[b,**], Morteza Nejati[c,**]

[a]*Department of Civil Engineering and Applied Mechanics, McGill University, Montréal, QC, Canada H3A 0C3*
[b]*Swiss seismological service (SED) at ETH Zurich, Switzerland*
[c]*Department of Earth Sciences, ETH Zurich, Switzerland*

Abstract

This paper presents an alternative approach for estimating the Biot coefficient for the Grimsel granite, which appeals to the multi-phasic mineralogical composition of the rock. The modelling considers the transversely isotropic nature of the rock that is evident from both the visual appearance of the rock and determined from mechanical testing. Conventionally, estimation of the compressibility of the solid material is performed by fluid saturation of the pore space and pressurization. The drawback of this approach in terms of complicated experimentation and influences of the unsaturated pore space is alleviated by adopting the methods for estimating the solid material compressibility using developments in theories of multiphase materials. The results of the proposed approach are compared with estimates available in the literature.

Keywords: Biot coefficient, transversely isotropic rocks, compressibility of the solid materials, Walpole bounds, Voigt-Reuss-Hill estimates

1. Introduction

The classical theory of poroelasticity proposed by Biot (1941) is a major contribution to the disciplines of geosciences and geomechanics with applications that include porous earth materials saturated by fluids. The studies in this area are numerous and no attempt will be made to provide a comprehensive survey of past and recent developments. Advances in the area of poroelasticity, and its applications to problems in geomechanics in particular are given by Rice and Cleary (1976); Yue and Selvadurai (1995); Selvadurai (1996, 2007); Wang (2000); Verruijt (2015); Cheng (2015); Selvadurai et al. (2015); Selvadurai and Suvorov (2016) and others. The basic development of the classical theory of poroelasticity relies on constitutive assumptions of Hookean elastic behaviour of the porous skeleton and Darcy flow through the porous medium. In addition, an important component of the theory relates to the partitioning of the total stress tensor for the poroelastic solid between the stresses carried purely by the porous skeleton and the stresses carried by the pore fluid. The partitioning is an important component in the theory of poroelasticity that allows the time-dependent shedding of the applied stresses from the pore fluid to the porous skeleton. The stresses sustained by the porous skeleton have important consequences to the definition of failure of the poroelastic material either through the development of damage (Selvadurai, 2004; Selvadurai and Shirazi, 2004, 2005; Selvadurai et al., 2015), or fracture development and boundary effects on heterogeneities (Selvadurai et al., 2011; Selvadurai and Głowacki, 2017, 2018)

*Corresponding author, William Scott Professor and Distinguished James McGill Professor
**Post-Doctoral Fellow
Email address: patrick.selvadurai@mcgill.ca (A.P.S. Selvadurai)

or plastic flow (Selvadurai and Suvorov, 2012, 2014). From an environmental geosciences perspective, alterations in the skeletal permeability associated with its damage can lead to enhanced migration of contaminants and hazardous materials. In Biot's theory, the partitioning of the total stress is achieved through consideration of the bulk modulus of the porous skeleton (K_D) and the bulk modulus of the solid material composing the porous skeleton (K_S), which introduces the Biot coefficient α and for an isotropic elastic skeleton, has the form $\alpha = 1 - (K_D/K_S)$. When the bulk modulus of solid material is large in comparison to the skeletal bulk modulus, $\alpha \to 0$, which is the conventional stress partitioning approach proposed in the theory of soil consolidation proposed by Terzaghi (1923). Unlike in soils, the Biot coefficient for rocks can be less than unity. If Biot's classical theory of poroelasticity is accepted, values of α cannot be greater than unity. Such a value would imply that either $K_D < 0$ or $K_S < 0$, which would violate the positive definiteness arguments for the strain energy of an elastic porous skeleton (Davis and Selvadurai, 1996; Selvadurai, 2000) with no locked-in self equilibrating stresses (i.e. the skeleton expands under compressive isotropic stresses). It should also be noted that the Biot coefficient as originally envisaged by Biot (1941) is a scalar parameter. Extension of the theory to consider an anisotropic skeletal fabric is admissible but the coefficient still remains a scalar parameter. A range of values for α is given by Detournay and Cheng (1993); Wang (2000); Cheng (2015).

The experimental procedure for determining the Biot coefficient α involves estimating the bulk modulus of the porous skeleton (K_D), which, in the case of an isotropic skeletal fabric, can be obtained by subjecting a dry or moisture free and jacketed specimen of the rock to isotropic compression and measuring the resulting volumetric strain. This is a straightforward experimental technique and the results can also be verified by conducting uniaxial compression tests on the isotropic rock and measuring both the Young's modulus and Poisson's ratio. The measurement of the compressibility of the solid material composing the skeletal fabric can be either straightforward or complicated depending on the permeability characteristics of the porous material. For rocks with relatively high permeability (e.g. Indiana limestone $10^{-13} \sim 10^{-15}\text{m}^2$ (Selvadurai and Glowacki, 2008; Selvadurai and Selvadurai, 2010, 2014), Vosges sandstone $\sim 10^{-13}\text{m}^2$ (Moulu et al., 1997), etc.), the pore space of the rock can be saturated by initiating a combination of steady flow and vacuum saturation. To determine the compressibility of the solid material, the confining isotropic stresses are allowed to nearly equilibrate with the pore fluid pressure and the volume changes measured can be used to estimate the compressibility of the solid material composing the porous fabric.

The ideal arrangement for the measurement of the K_S would involve an unjacketed specimen where the saturating fluid is identical to the pressurizing fluid. In situations where the saturating fluid is water and the pressurizing fluid is oil (needed to attain high pressures without compressibility issues), the sample needs to be jacketed. The sample can be subjected to a constant high confining pressure and the pore fluid pressure increased to attain equilibrium. This appears to be the preferred mode of estimation of the solid material compressibility provided the saturation of the pore space is assured with in the timeframe of a test. Other variations on this procedure are possible depending on the permeability of the rock under investigation. The article by Bemer et al. (2004) relating to the measurement of poroelastic parameters for the Meuse/Haute Marne argillites advocates the use of oedometric compression tests for the estimation of the Biot coefficient. If ever there is a criticism in the use of oedometric compression tests for estimating the Biot coefficient, this relates to the radial stress developed in the sample, which is a function of the skeletal Poissons ratio, which adds a level of uncertainty in the interpretation of the solid material compressibility. Also, the Meuse/Haute Marne argillite is a clay rock, which will have irreversible deformations in terms of the stress history and the interpretation of the skeletal elasticity properties should reflect stress history. In the case of the Grimsel granite, such effects are not expected to be significant.

With very low permeability materials (e.g. the Cobourg limestone $\sim 10^{-23}\text{m}^2$ to 10^{-19}m^2 (Selvadurai et al., 2011)),

the process of saturation of the pore space can take an inordinately long time with no assurance that the entire pore space is fully saturated or that there are no residual pore fluid pressure artifacts (Selvadurai, 2009). Furthermore, even if the pore space is saturated, attaining equalization of the externally applied pressure with the internal pore fluid pressure can take substantial time (for 150 mm diameter cylindrical Cobourg limestone samples, more than 100 days are required for saturation). For this reason, Selvadurai (2019) proposed an alternative approach where the compressibility of the solid material phase(s) can be estimated by considering the multi-phasic theories developed for estimating the effective properties of composite elastic materials. The composite material theories associated with the Voigt-Reuss-Hill estimates (Voigt, 1928; Reuss, 1929; Hill, 1952, 1965) and the upper and lower bound estimates proposed by Hashin and Shtrikman (1963) can be used to estimate the bulk modulus of the solid material (see also Walpole, 1966; Francfort and Murat, 1986). In this paper, we apply these basic concepts to determine the Biot coefficient for the Grimsel granite. This granite is encountered in the Underground Research Laboratory constructed in Grimsel, Switzerland, in order to perform heater experiments to simulate the thermo-hydro-mechanical (THM) loading associated with heat-emitting containers in the event that the site is chosen as a repository for the deep geologic disposal of high level nuclear fuel waste (i.e. the Full-scale Engineered Barriers EXperiment (FEBEX).) A typical section along the Grimsel Laboratory associated with the FEBEX heater experiment location is shown in Figure 1.

The Aar granitic rock (also referred to as Aare granitic rock) setting at Grimsel has been associated with initiatives related to the use of granitic rock formations as potential hosts for the creation of deep geologic repositories for the disposal of heat-emitting nuclear fuel waste. Detailed descriptions of the geological settings of the Aar massif of the Central Alps are given by several authors including Stalder (1964); Wüthrich (1965); Steck (1968); Schaltegger (1990b,a); Schaltegger and Corfu (1992) and references to further studies are given by Goncalves et al. (2012). Geo-scientific studies of the Aar granite have been conducted by a number of agencies including NAGRA and ENRESA and these initiatives are documented in several reports and articles by Amiguet (1985); Pahl et al. (1989); Keusen et al. (1989); Möri et al. (2003); Alonso and Alcoverro (2005); Alonso et al. (2005); Rabung et al. (2012); Bouffier (2015); Garralón et al. (2017); Krietsch et al. (2019). In relation to the FEBEX research experiments, the geological setting of the Grimsel Laboratory contains alternate layers of the Aar granite, transition zones and Granodiorite, separated by Lamprophyres and zones that are subjected to intense shearing. A typical view of the geological setting is shown in Figure 1. During the FEBEX experiments, the Grimsel Laboratory was used to conduct heater experiments where the heaters were encapsulated in bentonitic clay. An extensive program of research was conducted by a series of research groups to validate the THM response of both the bentonitic buffer and the rock mass and the results of the research efforts are documented by Alonso and Alcoverro (2005) and Alonso et al. (2005). The Grimsel granite used in this research investigation was obtained from boreholes PRP16.001 and INJ16.001 located in the southern part of the laboratory, drilled from the AU cavern. These boreholes were drilled as a part of the Grimsel In-situ Stimulation and Circulation (ISC) project (see the location in Figure 1) that investigated the seismo-hydro-mechanical response of the rock mass to hydraulic stimulation (Amann et al., 2018; Gischig et al., 2018; Doetsch et al., 2018; Jalali et al., 2018).

During the geological evolution of the Aar Massif, the strata acquired different mineralogical compositions and the studies by Schaltegger and Krähenbühl (1990) contain very detailed evaluations of the mineralogical compositions of rocks recovered from the Grimsel and Reuss regions. This information is valuable for estimating the solid material compressibility of the Grimsel granite and for distinguishing the sample locations. For example, the work of Jokelainen et al. (2013) provides information on the mineralogical composition of the Grimsel granodiorite and the

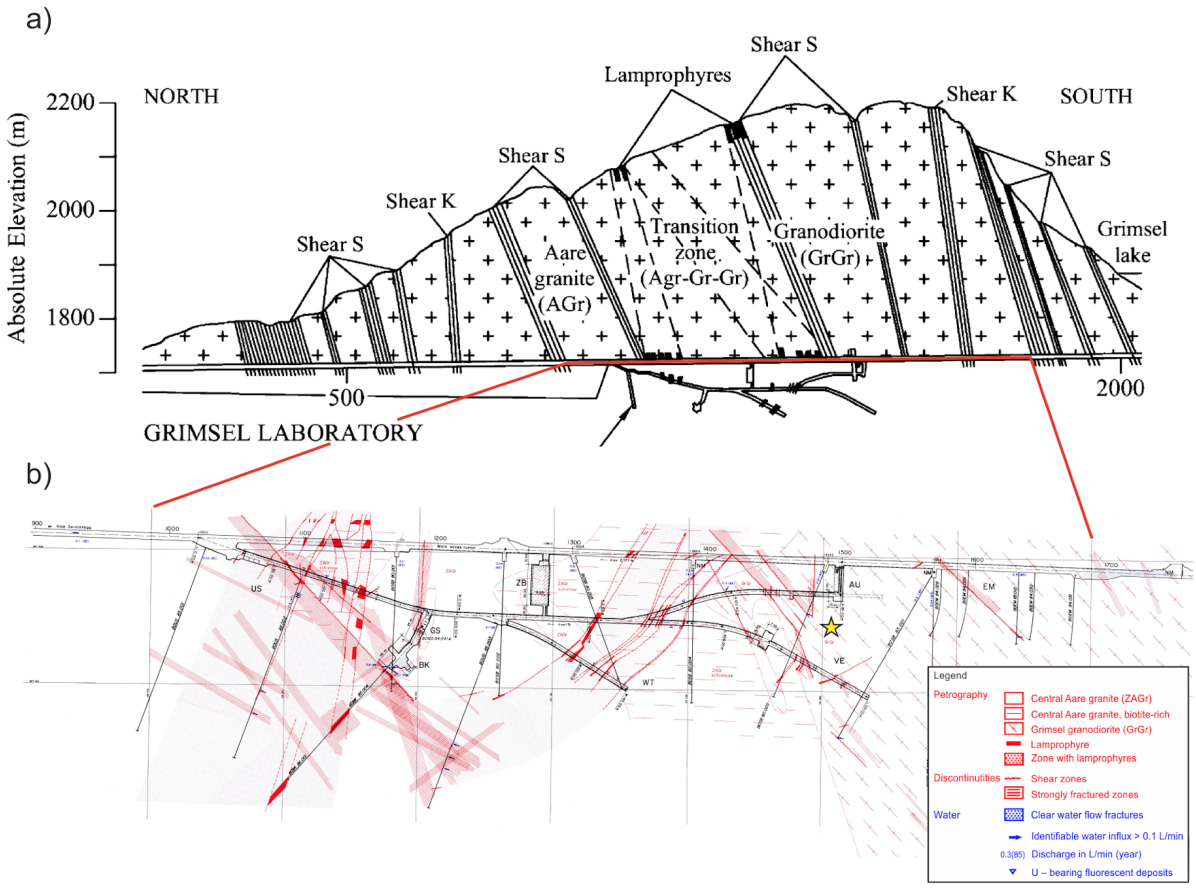

Figure 1: (a) The Grimsel Laboratory and the FEBEX Drift [After Alonso et al. (2005)]; (b) Detailed map view of the FEBEX drift for reference only [After Keusen et al. (1989) and from NAGRA Technical Report NTB87-14E].

study by Missana and Garcia-Gutiérrez (2012) provides the mineralogical composition of the FEBEX granite. The results reported in these investigations are summarized in Tables 1-4 for completeness.

Figure 2 shows cores of the Grimsel granite and, from a visual perspective, the rock has the appearance of stratifications that would point to the likely presence of transverse isotropy, in terms of its elasticity properties, fluid flow and fracture and failure characteristics.

The microstructure includes larger crystals of quartz (with dimensions up to 8 mm) and this requires that a suitable representative volume element is considered, both in the mechanical testing and mineralogical property evaluations. Extensive geomechanical characterization studies have been performed on the Grimsel granite and these are given in the references cited previously. Permeability studies are also reported by Schild et al. (2001). A comprehensive inter-laboratory study of permeability of the Grimsel granodiorite is also given in David et al. (2018a,b).

The objective of this study is to employ the existing data on the mechanical characterization of the transversely isotropic granite to estimate the skeletal compressibility of the granite and to use XRD studies of the mineralogical composition of the Grimsel granite to estimate the compressibility of the solid phase composing the porous fabric.

Table 1: Short Petrographical Descriptions of the Rock Samples Analyzed by Schaltegger and Krähenbühl (1990). Compositions are estimated from thin section, all=allanite; ap=apatite; bio=biotite; cc=calcite; chl=chlorite; ep=epidote; fluo=fluorite; gar=garnet; kfs=K-feldspar; leuc=leucoxene; op=opaques; plag=plagioclase; ser=sericite; sph=sphene; stilp = stilpnomelane; qtz = quartz; zir = zircon.

Sample No.	Rock Name	Mesoscopic description	Mineralogical composition
KAW 128	Northern Border Facies, Gurtnellen granite (Reuss valley)	leucocratic, massiv, coarse-grained granite	38% qtz, 35% kfs, 25% plag, 2% bio; ap, op, all, zir, gar, sph, ep, stilp, chl;
KAW 2213A	Grimsel Granodiorite Grimsel lake (Grimsel)	dark, coarse-grained granite to granodiorite, strongly foliated in most cases, augen texture; abundant dark enclaves	25% qtz, 25% kfs, 38% plag, 12%; bio; ap, op, sph, all, zir, chl, ep, ser, leuc, cc; plag cumulates
KAW 2219	Central Aar Granite s.s., main facies, Chuenzentennen (Grimsel)	coarse-grained granite with only slight cataclastic deformation	32% qtz, 29% kfs, 31% plag, 8% bio; ap, op, zir, all, leuc, chl, ser, ep
KAW 2220	Central Aar Granite s.s., leucocratic facies, Hangholz (Grimsel)	medium-grained granite, slightly foliated, occurring as stocks and schlieren within the main facies of the Central Aar Granite s.s.	34% qtz, 32% kfs, 28% plag, 6% bio; ap, op, zir, all, gar, chl, leuc, ser, ep
KAW 2408	Mittagflue Granite, Tschingel bridge (Grimsel)	leucocratic, massive, coarse-grained granite, analogous to the Northern Border Facies of the Reuss valley	35% qtz, 35% kfs, 28% plag, 2% bio; ap, zir, gar, all, chl, ep, stilp
KAW 2427	Central Aar Granite s.s., main facies, Gelmerstutz (Grimsel)	coarse-grained, massive granite	main rock-forming minerals as KAW 2219, op, all, sph, zir, ap,ep, ser
KAW 2518	Central Aar Granite s.l., Göschenen (Reuss valley)	leucocratic, medium-grained granite, massive to slightly foliated	32% qtz, 32% kfs, 32% plag, 4% bio; ap, ep, all, zir, gar, ser, leuc
KAW 2519	Central Aar Granite s.l., Schöllenen (Reuss valley)	dark, coarse-grained granodiorite with moderate foliation, augen texture	27% qtz, 35% plag, 28% kfs, 10% bio; all, zir, op, ap, sph, ep, leuc, chl
KAW 2521	Central Aar Granite s.l. Schöllenen (Reuss valley)	coarse-grained granodiorite, strongly foliated, similar to KAW 2519	zir, op, ap, sph, ep, leuc, chl same rock-forming minerals as KAW 2519
KAW 2529	Kessiturm Aplite, white facies (Grimsel)	fine-grained, aplitic (leucogranitic) intrusion of 200 × 800 m within the Grimsel Granodiorite	40% qtz, 35% kfs, 24% plag, 1% bio; zir, gar, op, fluo, leuc, chl, ep
KAW 2532	Kessiturm Aplite, grey facies (Grimsel)	fine-grained grey aplite, forming blobs and schlieren within the white Kessiturm aplite	40% qtz, 30% kfs, 28% plag, 2% bio; gar, chl, ep, ser

2. Skeletal Bulk Modulus of the Grimsel Granite

The fabric of the Grimsel granite is indicative of a transversely isotropic material (Nejati, 2018; Dutler et al., 2018; Dambly et al., 2019; Nejati et al., 2019). The elastic stress-strain relationships for a transversely isotropic material can be expressed in several forms (see e.g. Hearmon, 1961; Lekhnitskii, 1963; Ting, 1996). We consider the case where the plane of isotropy (x, y) of the transversely isotropic elastic material is normal to the z-axis. The equations of elasticity governing the normal strains can be written in the forms

$$\begin{aligned}
\epsilon_{xx} &= \frac{\sigma_{xx}}{E_x} - \frac{\nu_{yx}\sigma_{yy}}{E_y} - \frac{\nu_{zx}\sigma_{zz}}{E_z} \\
\epsilon_{yy} &= -\frac{\nu_{xy}\sigma_{xx}}{E_x} + \frac{\sigma_{yy}}{E_y} - \frac{\nu_{zy}\sigma_{zz}}{E_z} \\
\epsilon_{zz} &= -\frac{\nu_{xz}\sigma_{xx}}{E_x} - \frac{\nu_{yz}\sigma_{yy}}{E_y} + \frac{\sigma_{zz}}{E_z}
\end{aligned} \tag{1}$$

We point out that the Poisson's ratio is generally defined as $\nu_{ij} = -\epsilon_j/\epsilon_i$ for a stress in the i direction. From Betti's reciprocal theorem,

Table 2: Geochemical Descriptions of the Rock Samples Across the Grimsel Test Site given by Keusen et al. (1989).

	Central Aare granite					**Grimsel-Granodiorite**					
	SB1	SB2	SB2	SB3	SB4	SB5	SB5	SB6	SB6	SB6	SB5
	74.98	14.00	74.00	93.00	72.20	35.96	39.20	48.98	59.00	75.97	39.20
	Wt.%	Wt.%	Wt.%	Wt.%	Wt.%	Wt.%	Wt.%	Wt.%	Wt.%	Wt.%	Wt.%
SiO_2	74.65	69.56	74.67	68.65	71.22	67.95	67.76	69.9	65.35	66.57	66.66
TiO_2	0.2	0.41	0.16	0.42	0.41	0.58	0.61	0.44	0.51	0.56	0.47
Al_2O_3	13.14	14.72	12.78	15.21	13.88	15.04	15.2	14.48	17.03	16.1	14.73
Fe_2O_3	1.39	2.98	1.13	2.97	2.6	3.44	3.58	2.71	3.3	3.61	4.1
MnO	0.04	0.1	0.04	0.09	0.07	0.07	0.07	0.06	0.08	0.08	0.09
MgO	0.24	0.69	0.18	0.69	0.56	1.27	0.54	0.76	0.91	0.88	0.12
CaO	1.01	2.08	0.93	1.97	1.84	1.85	1.29	1.71	2.56	2.83	6.99
Na_2O	3.88	4.52	3.69	4.59	3.87	4.01	4.57	3.98	4.9	4.84	3.95
K_2O	4.7	3.47	4.83	4.03	3.91	4.03	3.77	4.59	3.56	3.35	1.57
P_2O_3	0.07	0.13	0.05	0.13	0.12	0.19	0.19	0.14	0.16	0.18	0.15
Cr_2O_3	< 0.01	< 0.01	< 0.01	< 0.01	< 0.01	< 0.01	< 0.01	< 0.01	< 0.01	< 0.01	< 0.01
NiO	0.01	0.01	0.01	0.01	0.01	0.01	0.01	0.01	0.01	0.01	0.01
Loss of ign.	0.31	0.49	0.38	0.6	0.53	0.81	0.78	0.45	0.84	0.6	0.69
Ignition	98.92	99.15	98.84	99.35	99.01	99.24	99.36	99.22	99.2	99.6	99.52

Table 3: Mineralogical composition of the Grimsel Granodiorite (Gr-Gr) [After Jokelainen et al. (2013)].

Mineral	**Sample 1 (Volume %)**	**Sample 2 (Volume %)**
Plagioclase	39.0	34.0
Quartz	28.4	37.2
K-Feldspar	21.6	12.8
Biotite	5.0	7.8
Muscovite + sericite	2.6	1.6
Epidote	1.2	1.0
Amphibole	1.8	4.6
Chlorite	0.2	0.4
Titanate	-	0.6
Opaque minerals	0.2	-

$$\frac{\nu_{xy}}{E_x} = \frac{\nu_{yx}}{E_y}, \quad \frac{\nu_{xz}}{E_x} = \frac{\nu_{zx}}{E_z}, \quad \frac{\nu_{yz}}{E_y} = \frac{\nu_{zy}}{E_z} \tag{2}$$

Due to the isotropic behaviour in the xy plane, $E_x = E_y$, and $\nu_{zy} = \nu_{zx}$. These relations reduce the independent material constants needed to define the principal strains to four: E_x, E_z, ν_{xy} and ν_{zx}. Consider the situation where an element of the transversely isotropic elastic medium is subjected to an isotropic compressive stress state: $\sigma_{xx} = \sigma_{yy} = \sigma_{zz} = p$. The infinitesimal volumetric strain

$$\epsilon_v = \epsilon_{xx} + \epsilon_{yy} + \epsilon_{zz} = p\Big[\frac{2}{E_x}(1 - \nu_{xy}) + \frac{1}{E_z}(1 - 4\nu_{zx})\Big] \tag{3}$$

The skeletal bulk modulus for the transversely isotropic elastic material can be expressed in the form

$$K_D^{\mathrm{TI}} = \frac{p}{\epsilon_v} = \frac{E_x E_z}{2E_z(1 - \nu_{xy}) + E_x(1 - 4\nu_{zx})} \tag{4}$$

In terms of the elasticity parameters that are applicable to the direction normal to the planes of stratification (N) and directions along the planes of foliation or stratification (T), Eq. (4) can be written as

$$K_D^{\mathrm{TI}} = \frac{E_T E_N}{2E_N(1 - \nu_{TT}) + E_T(1 - 4\nu_{NT})} \tag{5}$$

In the limit of material isotropy, $E_N = E_T = E$ and $\nu_{TT} = \nu_{NT} = \nu$ and Eq. (5) reduces to the classical result

Table 4: Mineralogical composition of the FEBEX Granite [After Missana and Garcia-Gutiérrez (2012)].

Mineral	Volume (%)
Quartz	30-36
Plagioclase/Albite	19-23
K-Feldspar	31-37
Biotite-Chlorite	6-8
Muscovite	1-2

Figure 2: The Grimsel granite sample taken from the PRP1 borehole, with a diameter of 110 mm and a length of 240 mm. The nominal planes of stratification are inclined at about 50° to the axis of the sample.

$$K_D^{\mathrm{I}} = \frac{E}{3(1-2\nu)} \tag{6}$$

The estimation of the skeletal bulk modulus of the Grimsel granite can be attempted provided that the elasticity constants applicable to either an isotropic fabric or a transversely isotropic skeletal elastic behaviour, can be identified. The geomechanical investigations of the granitic rocks at Grimsel have ranged from the estimation of the deformability and strength characteristics of the rock to the assessment of the in situ stress state. The interpretation of the available data for estimating the *skeletal deformability characteristics* is complicated by the fact that the approaches used are not uniform and standardized; the earlier experimental studies may have deviated from currently acceptable standards (as suggested by ASTM and ISRM) for sample size, rate of loading, end restraints, method of interpretation of the experimental data for parameter extraction (secant modulus, tangent modulus, loading/unloading paths, cycles), etc. The exercise is also compounded by the material variability in terms of the Grimsel lithology and its influence on parameter variability. Within these limitations, attempts can be made to extract, from the existing literature, representative values of the elasticity characteristics of Grimsel granite with due consideration for the species of granite. The earliest record used in this study relates to the work of Amiguet (1985) and Alonso and Alcoverro (2005), which indicate the elasticity properties as $E \approx 60$ GPa; $\nu \approx 0.25$.

Pahl et al. (1989) used borehole dilatometer and overcoring to estimate the in-situ stress state and the overall deformability characteristics of the granite: $E \approx 40$ GPa; $\nu \approx 0.25$. The work of Keusen et al. (1989) gives a range of elasticity values applicable to the granodiorite ($max[E \approx 63$ GPa; $\nu \approx 0.48]$; $min[E \approx 32$ GPa; $\nu \approx 0.18]$) and the Aar granite ($max[E \approx 64$ GPa; $\nu \approx 0.49]$; $min[E \approx 42$ GPa; $\nu \approx 0.25]$). Ziegler and Amann (2012) also report the results of an extensive series of tests conducted on both wet and dry and coarse-grained and fine-grained samples of Grimsel granite. The results are presented as maximum and minimum values as follows: for the coarse-grained granite, $max[E \approx 59$ GPa; $\nu \approx 0.37]$; $min[E \approx 53$ GPa; $\nu \approx 0.25]$; for the medium-grained granite. The recent work

of Bouffier (2015) uses laboratory over coring techniques to estimate the deformability characteristics of the Grimsel granite and there is a wide range of results for both the elastic modulus and Poisson's ratio; average representative results are indicated by $E \approx 25$ GPa; $\nu \approx 0.33$. The work of Kant et al. (2017) is primarily focused on the estimation of the thermal properties of the Aar granite. The results they cite for the modulus of elasticity and Poisson's ratio are directly obtained from the work of Alonso et al. (2005) or indirectly from Keusen et al. (1989). Wenning et al. (2018) report studies of permeabilty and seismic velocity anisotropy across a ductile to brittle transition zone in the Grimsel granite.

The skeletal compressibility is also an important parameter in the interpretation of transient hydraulic pulse tests for estimating the fluid transport properties of low permeability materials including granite and argillaceous limestones (Brace et al., 1968; Selvadurai and Carnaffan, 1997; Selvadurai and Selvadurai, 2014; Selvadurai and Najari, 2015). The elasticity properties were determined via dynamic measurements and the maximum and minimum values are as follows: $max[E \approx 95$ GPa; $\nu \approx 0.18]$; $min[E \approx 65$ GPa; $\nu \approx 0.15]$. Considering the nature of the ductile to brittle transmission zone under investigation and the dynamic nature of the tests, these estimates are far in excess of those for the intact material that is tested statically. Furthermore, the bulk modulus estimated from the maximum values of E and ν is in the range of 50 GPa, which is lower than the bulk modulus of mono-mineralic albite but exceeds that of quartz. The study by Krietsch et al. (2019) deals with the characterization of the in situ stress state at the Grimsel test site, using a range of experiments including overcoring and hydraulic fracturing. The investigations were extended to include transverse isotropy of the rock mass.

The elasticity parameters were inferred through a computational back analysis of the overcoring technique; these authors also provide a comparison with the results obtained by Bouffier (2015). An averaging procedure gives maximum estimates of the isotropic elasticity parameters as $E \approx 26$ GPa; $\nu \approx 0.33$. The use of the Grimsel Laboratory facility for the FEBEX experiment (Alonso and Alcoverro, 2005) provided a useful International Benchmarking exercise to validate THM modelling of clay buffer regions that could be used in high-level nuclear waste management endeavours. The international collaborative effort (Alonso et al., 2005) focused more on the behaviour of the clay barrier during heating from emplaced heaters and fluid influx from the Grimsel granite. In many of the research efforts for the FEBEX Project, the Grimsel granite served as a heat sink and the rock mechanics aspects perhaps received less emphasis (i.e. the modelling of the bentonitic clay under heating was considered to be the major objective of the research as opposed to the modelling of the Grimsel granite). Also, to enhance fluid influx, the Grimsel gallery was considered to be a fractured rock mass and modelling the Grimsel rock elasticity properties varied between the research groups participating in the FEBEX project, with very low estimates of the elasticity properties (Nguyen et al., 2005) to near intact rock properties derived from the original studies of Amiguet (1985) (see also Gens et al., 1998; Alonso and Alcoverro, 2005; Rutqvist et al., 2003; Dupray et al., 2013). For this reason, the elasticity properties of the Grimsel granite cited in the papers dealing with the FEBEX exercise are excluded from consideration.

The majority of the studies focusing on the evaluation of the deformability characteristics of the Grimsel granite deal with isotropic elastic modelling. The possible influences of either elastic anisotropy or elastic transverse isotropy were addressed in the earlier study by Pahl et al. (1989) in connection with the estimation of in situ stress states. In this particular study, there is no clear statement of the applicable value of the elasticity constants governing transverse isotropy of the Grimsel granite (the degree of anisotropy (E_T/E_N) does not exceed 1.25) and the study culminates in the adoption of the isotropic elasticity properties that were indicated previously. The research by Nejati (2018) and Nejati et al. (2019) deals with the estimation of the deformability characteristics of the Grimsel granite based on the transversely isotropic elastic model with principal directions aligned in the stratification planes and normal to

the planes (Figure 2). These studies indicate that the Grimsel granite tested also exhibited significant anisotropy and nonlinearity. In addition, due to nonlinear effects, the secant, tangent and average values of the Young's modulus can depend on the stress level at which the value is estimated.

If a range of elastic behaviour can be clearly defined and if the elastic constants governing transverse isotropy can be determined, then, as shown by Eq. (5), the bulk modulus applicable to the transversely isotropic material can be evaluated objectively. The studies conducted by Nejati (2018) and Nejati et al. (2019) provide the following estimates for the elastic constants governing the transversely isotropic elasticity model for the Grimsel granite: $E_N \approx 30$ GPa; $E_T \approx 47$ GPa; $\nu_{TT} \approx 0.20$ GPa; $\nu_{NT} \approx 0.10$ GPa, Finally, Krietsch et al. (2019) conducted a series of experiments on the ISC core plugs, using overcoring and external pressurization of the hollow samples. These authors also give results of uniaxial tests conducted on core plugs extracted either normal or parallel to the foliations (Figure 18 of their paper). These results can be used to estimate the E_N and E_T. From the results presented by Krietsch et al. (2019), the relevant elastic moduli can be summarized as follows: $E_N \approx 13$ GPa; $E_T \approx 35$ GPa. These investigations, however, cannot be used to estimate the values of ν_{TT} and ν_{NT}. Dambly et al. (2019) presented the results of a research program geared to estimate the transversely isotropic elasticity parameters from results of ultrasonic dynamic tests and static tests. Nejati et al. (2019) compared the static and dynamic values of the elastic constants at zero-confinement, and concluded that the dynamic moduli are significantly greater than the static ones. In this study we have not considered experimental results derived from dynamic testing; therefore, for consistency, any results derived from dynamic testing of the Grimsel granite have been excluded from further consideration. Considering the experimental evaluations available in the literature, the elasticity parameters applicable to the Grimsel granite are summarized in Table 5.

Table 5: Elasticity Properties for the Grimsel Granite with the corresponding K_D^{I} or K_D^{TI} values: $K_D^{\mathrm{I}} = E/3(1-2\nu)$, $K_D^{\mathrm{TI}} = E_T E_N/[2E_N(1-\nu_{TT}) + E_T(1-4\nu_{NT})]$; N signifies the direction normal to the planes of stratification and T signifies the directions along the planes of stratification.

Reference	Elasticity Type	Elastic Constants	K_D^{I} or K_D^{TI}
Amiguet (1985)	Isotropic	$E = 60$ GPa; $\nu = 0.25$	$K_D^{\mathrm{I}} \approx 40$ GPa
Pahl et al. (1989)	Isotropic	$E = 40$ GPa; $\nu = 0.25$	$K_D^{\mathrm{I}} \approx 27$ GPa
Keusen et al. (1989) (Granodiorite)	Isotropic	mean $E \approx 47$ GPa; $\nu \approx 0.33$	$(K_D^{\mathrm{I}})_{\mathrm{mean}} \approx 46$ GPa
Keusen et al. (1989) (Aar granite)	Isotropic	mean $E \approx 53$ GPa; $\nu \approx 0.37$	$(K_D^{\mathrm{I}})_{\mathrm{mean}} \approx 68$ GPa
Ziegler and Amann (2012) Type 1–coarse grained	Isotropic	mean $E \approx 38$ GPa; $\nu \approx 0.36$	$(K_D^{\mathrm{I}})_{\mathrm{mean}} \approx 45$ GPa
Ziegler and Amann (2012) Type 2–medium grained	Isotropic	mean $E \approx 43$ GPa; $\nu \approx 0.37$	$(K_D^{\mathrm{I}})_{\mathrm{mean}} \approx 55$ GPa
Bouffier (2015)	Isotropic	$E = 26$ GPa; $\nu = 0.33$	$K_D^{\mathrm{I}} \approx 25$ GPa
Dambly et al. (2019)	Isotropic	$E = 44$ GPa; $\nu = 0.2$	$K_D^{\mathrm{I}} \approx 24$ GPa
Krietsch et al. (2019)	Transversely Isotropic	$E_N \approx 13$ GPa; $E_T \approx 35$ GPa; $\nu_{TT} \approx 0.15$; $\nu_{NT} \approx 0.15$	$K_D^{\mathrm{TI}} \approx 13$ GPa
Nejati et al. (2019); Nejati (2018)	Transversely Isotropic	$E_N \approx 30$ GPa; $E_T \approx 47$ GPa; $\nu_{TT} \approx 0.2$; $\nu_{NT} \approx 0.1$	$K_D^{\mathrm{TI}} \approx 19$ GPa

3. Compressibility of the Solid Material Composing the Grimsel Granite Fabric

The skeletal material of the Grimsel granite consists of a variety of mineral phases including quartz, biotite, anorthite, augite, microcline and traces of pyrite and magnetite. The composition of these minerals were determined both at the XRD facilities at University of Montréal, QC, Canada and at the Department of Earth Sciences, Institute of Geology, ETH, Zurich (Wenning et al., 2018). The estimated volume fractions and the values for the bulk moduli and shear moduli are shown in Tables 6 and 7 respectively. The average volume fractions and the mineralogical compositions tend to vary and the estimated values are, in general, considered to be approximate. The results of the

XRD evaluations do not provide sufficient accuracy to group the tested rocks into either the Grimsel granodiorite or the FEBEX Grimsel categories. A very cursory comparison with the data provided in Tables 1 to 3 would suggest that the mineralogical compositions provided by Wenning et al. (2018) and indicated in Table 6 correspond to the Grimsel granodiorite and the results shown in Table 7 correspond to the FEBEX granite. For this reason, the XRD data derived from both laboratory evaluations (ETH and McGill) are retained in the estimations of the solid material compressibility K_S. Also, the void fraction (<< 1%) is neglected in the calculations. The values for the bulk moduli and shear moduli for the various minerals were obtained from published literature (Alexandrov et al., 1964; Anderson and Nafe, 1965; Carmichael, 1990; Sisodia and Verma, 1990; Moos et al., 1997; Redfern and Angel, 1999; Schilling et al., 2003; Zhu et al., 2007; Mavko et al., 2009; Lin, 2013).

Table 6: Mineralogical Fractions of the Grimsel Granite [Data obtained by Wenning et al. (2018), Institute of Geology, ETH, Zurich].

Mineral	Specific Gravity	%	K_S (GPa)	G_S (GPa)
Biotite & Phlogopite	2.72	10	77	42
Muscovite	2.70	5	61	41
Epidote	2.75	6	107	60
Albite	3.19	40	76	26
Feldspar	2.60	16	76	26
Quartz	2.72	23	38	45
		Σ 100		

Table 7: Mineralogical Fractions of the Grimsel Granite [Data obtained by the Earth Sciences Laboratory, University of Montréal].

Mineral	Specific Gravity	%	K_S (GPa)	G_S (GPa)
Quartz	2.72	46	38	45
Biotite	2.70	5	77	42
Anorthite	2.75	37	68	38
Augite	3.19	5	95	59
Microcline	2.60	7	52	36
		Σ 100		

In the multi-phasic approach, the objective is the determine the overall bulk modulus for the solid mineralogical phase by considering the bulk moduli for the separate mineral constituents and their volume fractions. The most widely used relationships are those by Voigt (1928) and Reuss (1929). The Voigt (^{V}) and the Reuss (^{R}) estimates are

$$
\begin{aligned}
(K_S)_I^V &= \sum_i^n V_i (K_S)_i, \qquad (K_S)_I^R = \left[\sum_i^n \frac{V_i}{(K_S)_i} \right]^{-1} \\
(G_S)_I^V &= \sum_i^n V_i (G_S)_i, \qquad (G_S)_I^R = \left[\sum_i^n \frac{V_i}{(G_S)_i} \right]^{-1} \\
& i = Qrtz, Biotite, Anorthite, Augite, Microcline, Voids \\
& I = \text{Data from Table 1 or Table 2}
\end{aligned}
\tag{7}
$$

The results given in Hill (1952, 1965) are the mean of the Voigt and Reuss estimates. This basic approach can be applied to estimate the effective bulk and shear moduli for the Grimsel granite: i.e.

$$
\begin{aligned}
(K_S)_I &= \frac{1}{2}\left[(K_S)_I^V + (K_S)_I^R \right], \qquad (G_S)_I = \frac{1}{2}\left[(G_S)_I^V + (G_S)_I^R \right] \\
& I = \text{Data from Table 1 or Table 2}
\end{aligned}
\tag{8}
$$

Using the mineralogical compositions obtained from XRD analyses given in Table 1, we have

$$(K_S)_1 = 65 \text{ GPa}, \qquad (G_S)_1 = 33 \text{ GPa} \tag{9}$$

and using the mineralogical compositions obtained from XRD analyses given in Table 2, we have

$$(K_S)_2 = 52 \text{ GPa}, \qquad (G_S)_2 = 48 \text{ GPa} \tag{10}$$

We consider the upper and lower bounds for a multi-phasic composite consisting of n phases developed by Walpole (1966). The effective bulk modulus K for the multi-phasic material can be written as

$$\left[\sum_{i=1}^{n}\left(\frac{V_i}{K_l^* + K_i}\right)\right]^{-1} - K_l^* \le K \le \left[\sum_{i=1}^{n}\left(\frac{V_i}{K_g^* + K_i}\right)\right]^{-1} - K_g^* \tag{11}$$

where

$$K_l^* = \frac{4}{3}G_l, \qquad K_g^* = \frac{4}{3}G_g \tag{12}$$

In Eq. (12), G_l and G_g are, respectively, the lowest and greatest values of the shear modulus of the n phases. For completeness, we also record here the bounds for the effective shear modulus (G) of the n phasic mixture, which can be written as

$$\left[\sum_{i=1}^{n}\left(\frac{V_i}{G_l^* + G_i}\right)\right]^{-1} - G_l^* \le G \le \left[\sum_{i=1}^{n}\left(\frac{V_i}{G_g^* + G_i}\right)\right]^{-1} - G_g^* \tag{13}$$

where

$$G_l^* = \frac{3}{2}\left(\frac{1}{G_l} + \frac{10}{9K_l + 8G_l}\right)^{-1}, \quad G_g^* = \frac{3}{2}\left(\frac{1}{G_g} + \frac{10}{9K_g + 8G_g}\right)^{-1} \tag{14}$$

and K_l and K_g are, respectively, the lowest and greatest values of the bulk modulus of the n phases.

Considering the multiphasic data set given in Tables 6 and 7 , respectively

$$(K_S)_1 \in (64.6, 65.9)\,\text{GPa}, \quad (K_S)_2 \in (52.1, 52.7)\,\text{GPa} \tag{15}$$

Considering the range of solid material compressibilities obtained from the two laboratory investigations we can conclude that the lower (^{L}) and upper (^{U}) estimates for K_S are approximately

$$K_S^L \approx 52\,\text{GPa}, \quad K_S^U \approx 66\,\text{GPa} \tag{16}$$

The results for the skeltal compressibilities given in Table 5 can be combined with the range of solid material compressibilities to estimate the *upper* and *lower* limits of the Biot coefficient applicable to each estimate of K_D^{I} and K_D^{TI}. The relevant results are shown in Table 8. It may be noted that the composite materials approach outlined here has been used in the geomechanics and geosciences areas and references to these can be found in the volumes by Ahrens (1995); Markov and Preziosi (2000); Mavko et al. (2009) and in the articles by Suvorov and Selvadurai (2011) and Selvadurai (2019).

Table 8: Upper and lower limits for the Biot coefficient for the Grimsel Granite; $\alpha_U = 1-(K_D^{\mathrm{I}}$ or $K_D^{\mathrm{TI}})/K_S^U$, $\alpha_L = 1-(K_D^{\mathrm{I}}$ or $K_D^{\mathrm{TI}})/K_S^L$, $K_S^L \approx 52$ GPa, $K_S^U \approx 66$ GPa.

Reference	**Elasticity Type**	K_D^{I} or K_D^{TI}	α_L	α_U
Amiguet (1985)	Isotropic	$K_D^{\mathrm{I}} \approx 40$ GPa	0.23	0.39
Pahl et al. (1989)	Isotropic	$K_D^{\mathrm{I}} \approx 27$ GPa	0.48	0.59
Keusen et al. (1989) (Granodiorite)	Isotropic	$(K_D^{\mathrm{I}})_{mean} \approx 46$ GPa	0.12	0.30
Keusen et al. (1989) (Aar granite)	Isotropic	$(K_D^{\mathrm{I}})_{mean} \approx 68$ GPa	-0.31	-0.03
Ziegler and Amann (2012) Type 1–coarse grained	Isotropic	$(K_D^{\mathrm{I}})_{mean} \approx 45$ GPa	0.13	0.32
Ziegler and Amann (2012) Type 2–medium grained	Isotropic	$(K_D^{\mathrm{I}})_{mean} \approx 55$ GPa	-0.06	0.17
Bouffier (2015)	Isotropic	$K_D^{\mathrm{I}} \approx 25$ GPa	0.52	0.62
Dambly et al. (2019)	Isotropic	$K_D^{\mathrm{I}} \approx 24$ GPa	0.54	0.64
Krietsch et al. (2019)	Transversely Isotropic	$K_D^{\mathrm{TI}} \approx 13$ GPa	0.75	0.80
Nejati et al. (2019); Nejati (2018)	Transversely Isotropic	$K_D^{\mathrm{TI}} \approx 19$ GPa	0.63	0.71

4. Discussion

In theories developed for estimating the elasticity of multi-phasic materials, the most extensive studies relate to two-component elastic materials. Theories, however, have also been developed by several researchers to include a distribution of three elastic phases in the composite material. An early study in this area is by Cohen and Ishai (1967) that considered the presence of a large voids content in the two-phase system. Several other developments have been proposed in the literature references to studies are given by Selvadurai (2019) and the other references cited in the introduction. The extension to three elastic phases was also presented in the studies by Talbot et al. (1995) and, more recently, by Lin and Ju (2009).

Here we have used the theoretical estimates proposed by Vogt and Reuss and modified by Hill, and the bounds proposed by Walpole to estimate the upper and lower bound values for the effective bulk moduli of the solid phase. It is shown that the estimates proposed by Voigt-Reuss-Hill and those of Walpole yield practically the same values. The results of the evaluations presented in the paper would suggest that the multiphasic approach in conjunction with XRD data provides a useful alternative to validating the conventional experimental approach for estimating the solid material composing low permeability porous media. The skeletal bulk moduli for the Grimsel granite shows a wide variation, indicative of variable lithology of the igneous rock formation. In this sense, it is prudent to assume a set of limits for the choice of the Biot coefficient rather than to assign a specific value. Certain data obtained in this study give rise to non-realistic values of the Biot coefficient, clearly arising from the estimation of the skeletal compressibility.

As a guide, experimental results for the skeletal compressibility values that exceed the effective solid material compressibility of the minerals with the largest volume fractions should be disregarded. Therefore these results can be excluded without further comment. (i.e. Since the multi-phasic assessment of the compressibility of the solid material has a lower limit of approximately $K_S^L \approx 50$ GPa, plausible values of the Biot coefficient will be obtained when $K_D < K_S$.) Also, excessively low values of K_D need to be re-examined before using the data to estimate the Biot coefficient. Excessively low values can result from inaccurate estimation of the elastic modulus and Poisson's ratio. Similarly, excessively high values of the skeletal stiffness can result from inaccurate estimates of the Poisson's ratio of the rock. For example, if samples are loaded in the direction of the foliations or stratifications, micro-crack or defect development during compression can give rise to lateral deformations that can be a result of void/crack generation and not a result of material deformation. Considering the numerical values presented in Table 8, and the above comments, several estimates for the Biot coefficients can be excluded from further discussion. The Table 9

summarizes the revised set of realistic experimental estimates for the Biot coefficient of the Grimsel granite, taking into consideration the aforementioned caveats on the experimental results. Within the context of Biot's theory of poroelasticity, the deformability of the skeletal fabric and the constituent solids is always assumed to be linearly elastic. The developments can also be extended to include elasto-plastic behaviour of the porous skeleton (Suvorov and Selvadurai, 2019).

Table 9: Reduced Data Set for the Upper and Lower Limits for the Biot coefficient for the Grimsel Granite.

Reference	**Elasticity Type**	K_D^{I} or K_D^{TI}	α_L	α_U
Pahl et al. (1989)	Isotropic	$K_D^{\mathrm{I}} \approx 27\,\mathrm{GPa}$	0.48	0.59
Bouffier (2015)	Isotropic	$K_D^{\mathrm{I}} \approx 25\,\mathrm{GPa}$	0.52	0.62
Dambly et al. (2019)	Isotropic	$K_D^{\mathrm{I}} \approx 24\,\mathrm{GPa}$	0.54	0.64
Nejati et al. (2019); Nejati (2018)	Transversely Isotropic	$K_D^{\mathrm{TI}} \approx 19\,\mathrm{GPa}$	0.63	0.71

5. Conclusions

The accurate estimation of the skeletal deformability characteristics of a porous rock is an essential pre-requisite for the estimation of the Biot coefficient for a fluid-saturated poroelastic material. While the procedures for conducting the either uniaxial or triaxial tests for estimation the skeletal deformability characteristics is well known, the exact procedure for estimating the elastic moduli, Poisson's ratio, etc., needs to be better documented so that the interpretations of experimental data can be consistent. The conventional procedure for the pressurization of a saturated sample of the rock and the measurement of the resulting sample strains when the externally applied cell pressure matches the pore fluid pressure is perhaps the best procedure for estimating the compressibility of the solid phases of the porous medium. This, however, is not a routine procedure for low permeability materials and substantial pressures need to be applied to ensure that volumetric strains of an accurately measurable value can be recorded. Also, in such cases the strains could involve irreversible grain boundary frictional slip and this needs to be excluded from the estimation of the solid material compressibility.

Here, we advocate the use of a multiphasic approach where the theories of composite materials can be used to estimate the compressibility of the solid material composing the porous skeleton. This is a relatively easy approach since XRD evaluations of the mineralogical phase composition are usually carried out to characterize the rock. In relation to the Grimsel granite, the analysis points to a Biot coefficient that has bounds rather than a specific value: i.e. $0.48 < \alpha < 0.71$. Values for the Biot coefficient for other types of rocks include the following [see also Table 1 in Detournay and Cheng (1993)]: Westerly granite ($\alpha \approx 0.47$). Values for the Biot coefficient for other types of granite in Manitoba, Canada, a value of $\alpha = 0.73$ is cited (Lau and Chandler, 2004); Sandstones have also shown this same variability: Ruhr sandstone ($\alpha \approx 0.65$), Berea sandstone ($\alpha \approx 0.79$), Weber sandstone ($\alpha \approx 0.64$), Ohio ($\alpha \approx 0.65$), Pecos sandstone ($\alpha \approx 0.83$) and Boise sandstone ($\alpha \approx 0.85$) [Further estimates are provided by Zimmerman (1991)]; Cobourg limestone ($\alpha \approx 0.66$). With soft rocks such as chalk, the Biot coefficient is invariably in the range 0.80 to 1.0 (Alam et al., 2010; Nermoen et al., 2013). For the Callovo -Oxfordian claystone the Biot coefficient is estimated to be in the range of 0.84 (Belmokhtar et al., 2018). Biot coefficient for gas-bearing tight sandstone is estimated at $\alpha \approx 0.38$ (Selvadurai, 2019). Other estimates for a variety of rocks encountered in a coal mining setting are also given by Chen et al. (2019).

Acknowledgement

The work described in the paper was supported by a Discovery Research Grant awarded by the Natural Sciences and Engineering Research Council of Canada. This study is part of the In situ Stimulation and Circulation (ISC) project established by the Swiss Competence Center for Energy Research-Supply of Electricity (SCCER-SoE) with the support of Innosuisse. The authors are also grateful to Professor Eduardo Alonso (UPC, Spain), Professor Lyesse Laloui (EPFL, Switzerland), Professor Florian Amman (RWTH, Germany), Professor Martin Mazurek (University of Bern, Switzerland), Dr. Stratis Vomvoris (NAGRA, Switzerland), Professor Christian David (Université Cergy-Pontoise, France), Dr. Jonny Rutqvist (LBNL, USA), Dr. Farid Laouafa (INERIS, France) and Dr. Son Nguyen (CNSC, Canada) and Professor R.W. Zimmerman (Imperial College, UK) for helpful comments. The authors gratefully acknowledge the comments made by Dr. Joseph Doetsch, Institute of Geophysics, Department of Earth Sciences ETH Zurich, which led to improvements in the presentation. The authors, however, are entirely responsible for the statements and conclusions presented in the paper. Finally, the authors are grateful to the reviewers for their highly constructive comments that led to improvements in the presentation.

References

Ahrens, T. J., 1995. Rock Physics and Phase Relations: A Handbook of Physical Constants. American Geophysical Union, Washington, DC.

Alam, M. M., Borre, M. K., Fabricius, I. L., Hedegaard, K., Røgen, B., Hossain, Z., Krogsbøll, A. S., 2010. Biot's coefficient as an indicator of strength and porosity reduction: Calcareous sediments from Kerguelen Plateau. Journal of Petroleum Science and Engineering 70 (3-4), 282–297.

Alexandrov, K. S., Rhyzova, T. V., Beliko, B. P., 1964. The elastic properties of pyroxenes. Soviet Physics-Crystallography 8, 589–591.

Alonso, E. E., Alcoverro, J., 2005. DECOVALEX III PROJECT. Modelling of FEBEX In-Situ Test, Task 1 Final Report. Tech. rep., SKI Report 2005:20.

Alonso, E. E., Alcoverro, J., Coste, F., Malinsky, L., Merrien-Soukatchoff, V., Kadiri, I., Nowak, T., Shao, H., Nguyen, T. S., Selvadurai, A. P. S., Armand, G., Sobolik, S. R., Itamura, M., Stone, C. M., Webb, S. W., Rejeb, A., Tijani, M., Maouche, Z., Kobayashi, A., Kurikami, H., Ito, A., Sugita, Y., Chijimatsu, M., Börgesson, L., Hernelind, J., Rutqvist, J., Tsang, C. F., Jussila, P., 2005. The FEBEX benchmark test: Case definition and comparison of modelling approaches. International Journal of Rock Mechanics and Mining Sciences 42, 611–638.

Amann, F., Gischig, V., Evans, K., Doetsch, J., Jalali, R., Valley, B., Krietsch, H., Dutler, N., Villiger, L., Brixel, B., Klepikova, M., Kittilä, A., Madonna, C., Wiemer, S., Saar, M. O., Loew, S., Driesner, T., Maurer, H., Giardini, D., 2018. The seismo-hydromechanical behavior during deep geothermal reservoir stimulations: open questions tackled in a decameter-scale in situ stimulation experiment. Solid Earth 9 (1), 115–137.

Amiguet, J.-L., 1985. Grimsel Test Site. Felskennwerte von intaktem Granit. Zusammenstellung felsmechanischer Laborresultate diverser granitischer Gesteine. Tech. rep., NAGRA, NIB 85-08.

Anderson, O. L., Nafe, J. E., 1965. The bulk modulus-volume relationship for oxide compounds and related geophysical problems. Journal of Geophysical Research 70 (16), 3951–3963.

Belmokhtar, M., Delage, P., Ghabezloo, S., Conil, N., 2018. Drained Triaxial Tests in Low-Permeability Shales: Application to the Callovo-Oxfordian Claystone. Rock Mechanics and Rock Engineering 51 (7), 1979–1993.

Bemer, E., Longuemare, P., Vincké, O., 2004. Poroelastic parameters of Meuse/Haute Marne argillites: Effect of loading and saturation states. Applied Clay Science 26 (1-4), 359–366.

Biot, M. A., 1941. General theory of three-dimensional consolidation. Journal of Applied Physics 12 (2), 155–164.

Bouffier, C., 2015. Stress measurements by overcoring at the Grimsel site. Results from the campaign of August-September 2015 Study Report. Tech. rep., ETH Zurich, https://doi.org/10.3929/ethz-b-000256660.

Brace, W., Walsh, J., Frangos, W., 1968. Permeability of Granite under High Pressure. Journal of Geophysical Research 73 (6), 2225–2236.

Carmichael, R. S., 1990. Practical Handbook of Physical Properties of Rocks and Minerals. CRC Press, Boca Raton, FL.

Chen, Y., Selvadurai, A. P. S., Liang, W., 2019. Computational Modelling of Groundwater Inflow During a Longwall Coal Mining Advance: A Case Study from the Shanxi Province, China. Rock Mechanics and Rock Engineering 52 (3), 917–934.

Cheng, A. H. D., 2015. Poroelasticity. Springer-Verlag, Berlin.

Cohen, L., Ishai, O., 1967. The elastic properties of three-phase composites. Journal of Composite Materials 1, 390–403.

Dambly, M., Nejati, M., Vogler, D., Saar, M. O., 2019. On the direct measurement of the shear moduli in transversely isotropic rocks using the uniaxial compression test. International Journal of Rock Mechanics and Mining Sciences 113, 220–240.

David, C., Wassermann, J., Amann, F., Klaver, J., Davy, C., Sarout, J., Esteban, L., Rutter, E. H., Hu, Q., Louis, L., Delage, P., Lockner, D. A., Selvadurai, A. P. S., Vanorio, T., Hildenbrand, A. A., Meredith, P. G., Browning, J., Mitchell, T. M., Madonna, C., Billiotte, J., Reuschlé, T., Lasseux, D., Fortin, J., Lenormand, R., Loggia, D., Nono, F., Boitnott, G., Jahns, E., Fleury, M., Berthe, G., Braun, P., Grégoire, D., Perrier, L., Polito, P., Jannot, Y., Sommier, A., Krooss, B., Fink, R., Clark, A., 2018a. KG2B, a collaborative benchmarking exercise for estimating the permeability of the Grimsel granodiorite-Part 2: Modelling, microstructures and complementary data. Geophysical Journal International 215 (2), 825–843.

David, C., Wassermann, J., Amann, F., Lockner, D. A., Rutter, E. H., Vanorio, T., Hildenbrand, A. A., Billiotte, J., Reuschlé, T., Lasseux, D., Fortin, J., Lenormand, R., Selvadurai, A. P. S., Meredith, P. G., Browning, J., Mitchell, T. M., Loggia, D., Nono, F., Sarout, J., Esteban, L., Davy, C., Louis, L., Boitnott, G., Madonna, C., Jahns, E., Fleury, M., Berthe, G., Delage, P., Braun, P., Grégoire, D., Perrier, L., Polito, P., Jannot, Y., Sommier, A., Krooss, B., Fink, R., Hu, Q., Klaver, J., Clark, A., 2018b. KG2B, a collaborative benchmarking exercise for estimating the permeability of the Grimsel granodiorite - Part 1: Measurements, pressure dependence and pore-fluid effects. Geophysical Journal International 215 (2), 799–824.

Davis, R. O., Selvadurai, A. P. S., 1996. Elasticity and Geomechanics. Cambridge University Press, Cambridge.

Detournay, E., Cheng, A. H. D., 1993. Comprehensive rock engineering: Principles, practice and projects. In: Hudson JA, ed., Fundamentals of Poroelasticity, vol. 1. Pergamon Press, Oxford.

Doetsch, J., Gischig, V., Villiger, L., Krietsch, H., Nejati, M., Amann, F., Jalali, M., Madonna, C., Maurer, H., Wiemer, S., Driesner, T., Giardini, D., 2018. Subsurface fluid pressure and rock deformation monitoring using seismic velocity observations. Geophysical Research Letters, Accepted for publication.

Dupray, F., François, B., Laloui, L., 2013. Analysis of the FEBEX multi-barrier system including thermoplasticity of unsaturated bentonite. International Journal for Numerical and Analytical Methods in Geomechanics 37, 399–422.

Dutler, N., Nejati, M., Valley, B., Amann, F., Molinari, G., 2018. On the link between fracture toughness, tensile strength, and fracture process zone in anisotropic rocks. Engineering Fracture Mechanics 201, 56–79.

Francfort, G. A., Murat, F., 1986. Homogenization and optimal bounds in linear elasticity. Archive for Rational Mechanics and Analysis 94 (4), 307–334.

Garralón, A., Gómez, P., Turrero, M. J., Torres, E., Buil, B., Pea, J., 2017. Hydrogeochemical characterization of the groundwater in the FEBEX gallery, National Cooperative for the Disposal of Radioactive Waste. Tech. rep., NAGRA Arbeitsbericht, NAB 16-14, Wettingen, Switzerland.

Gens, A., Garcia-Molina, A. J., Olivella, S., Alonso, E. E., Huertas, F., 1998. Analysis of a full scale in situ testing simulating repository conditions. International Journal for Numerical and Analytical Methods in Geomechanics 22 (7), 515–548.

Gischig, V. S., Doetsch, J., Maurer, H., Krietsch, H., Amann, F., Frederick Evans, K., Nejati, M., Jalali, M., Valley, B., Christine Obermann, A., Wiemer, S., Giardini, D., 2018. On the link between stress field and small-scale hydraulic fracture growth in anisotropic rock derived from microseismicity. Solid Earth 9 (1), 39–61.

Goncalves, P., Oliot, E., Marquer, D., Connolly, J. A., 2012. Role of chemical processes on shear zone formation: An example from the grimsel metagranodiorite (Aar massif, Central Alps). Journal of Metamorphic Geology 30 (7), 703–722.

Hashin, Z., Shtrikman, S., 1963. A variational approach to the theory of the elastic behaviour of multiphase materials. Journal of the Mechanics and Physics of Solids 11 (42), 127–140.

Hearmon, R. F. S., 1961. An Introduction to Applied Anisotropic Elasticity. Clarendon Press, Oxford.

Hill, R., 1952. The elastic behaviour of a crystalline aggregate. Proceedings of the Physical Society A 65, 349–354.

Hill, R. R., 1965. A self-consistent mechanics of composite materials. Journal of the Mechanics and Physics of Solids 13, 213–222.

Jalali, M., Gischig, V., Doetsch, J., Naf, R., Krietsch, H., Klepikova, M., Amann, F., Giardini, D., 2018. Transmissivity changes and microseismicity induced by smallscale hydraulic fracturing tests in crystalline rock. Geophysical Research Letters 45, 2265–2273.

Jokelainen, L., Meski, T., Lindberg, A., Soler, J. M., Siitari-Kauppi, M., Martin, A., Eikenberg, J., 2013. The determination of 134Cs and 22Na diffusion profiles in granodiorite using gamma spectroscopy. Journal of Radioanalytical and Nuclear Chemistry 295 (3), 2153–2161.

Kant, M. A., Ammann, J., Rossi, E., Madonna, C., Höser, D., Rudolf von Rohr, P., 2017. Thermal properties of Central Aare granite for temperatures up to 500C: Irreversible changes due to thermal crack formation. Geophysical Research Letters 44 (2), 771–776.

Keusen, H., Ganguin, J., Schuler, P., Buletti, M., 1989. Technical report 87-14 E: Grimsel test site geology. Tech. rep., GEOTEST: Zollikofen / Bern.

Krietsch, H., Gischig, V., Evans, K., Doetsch, J., Dutler, N. O., Valley, B., Amann, F., 2019. Stress Measurements for an In Situ Stimulation Experiment in Crystalline Rock: Integration of Induced Seismicity, Stress Relief and Hydraulic Methods. Rock Mechanics and Rock Engineering 52 (2), 517–542.

Lau, J. S. O., Chandler, N. A., 2004. Innovative laboratory testing. International Journal of Rock Mechanics and Mining Sciences 41, 1427–1445.

Lekhnitskii, S. G., 1963. Theory of Elasticity of an Anisotropic Elastic Body. Holden-Day, San Francisco.

Lin, C. C., 2013. Elasticity of calcite: Thermal evolution. Physics and Chemistry of Minerals 40 (2), 157–166.

Lin, P. J., Ju, J. W., 2009. Effective elastic moduli of three-phase composites with randomly located and interacting spherical particles of distinct properties. Acta Mechanica 208 (1-2), 11–26.

Markov, K., Preziosi, L., 2000. Heterogeneous Media. Birkhauser-Verlag, Boston.

Mavko, G. M., Mukerji, T., Dvorkin, J., 2009. The Rock Physics Handbook, Tools for Seismic Analysis of Porous Media. Cambridge University Press, Cambridge.

Missana, T., Garcia-Gutiérrez, M., 2012. Comparison of the Cesium adsorption on different crystalline rocks, in 1st Workshop Proceedings of the Collaborative Project Crystalline Rock Retention Processses, (7th EC FP CP CROCK) (Rabung, T., Molinero, J., Garcia, D., Montoya, V., Eds). KIT Scientific Publishing, Barcelona, Spain.

Moos, D., Dvorkin, J., Hooks, A. J., 1997. Application of theoretically derived rock physics relationships ¢ Los Angeles " Critical porosity ". Geophysical Research Letters 24 (3), 329–332.

Möri, A., Mazurek, M., Adler, M., Schild, M., Siegesmund, S., Vollbrecht, A., Ota, K., Ando, T., Alexander, R., Smith, P. A., Haag, P., C., B., 2003. The Nagra-JNC in situ study of safety relevanr radionuclide retardation in fractured crystalline rock. IV: The in situ study of matrix porosity in the vicinity of a water conducting fracture. Tech. rep., NAGRA Technical Report, 00-08, Baden, Switzerland.

Moulu, J. C., Kalaydjian, F., Tsakiroglou, C. D., Burganos, V. N., Payatakes, A. C., Yao, J., Thovert, J.-F., Adler, P.-M., 1997. Characterization, reconstruction and transport properties of the Vosges sandstone. Revue de L'Institut Francais du Petrole 52, 3–21.

Nejati, M., 2018. On the anisotropy of mechanical properties in Grimsel granodiorite. Tech. rep., ETH Zurich, https://doi.org/10.3929/ethz-b-000289969.

Nejati, M., Dambly, M., , Saar, M. O., 2019. A methodology to determine the elastic properties of anisotropic rocks from a single uniaxial compression test. Journal of Rock Mechanics and Geotechnical Engineering, Accepted for publication.

Nermoen, A., Korsnes, R., Christensen, H. F., Trads, N., Hiorth, A., Madland, M. V., 2013. Measuring the Biot stress coefficient and its implications on the effective stress estimate. Proc. 47th US Rock Mech./Geomech. Symposium, San Francisco, CA, USA, ARMA, 282.

Nguyen, T. S., Selvadurai, A. P. S., Armand, G., 2005. Modelling the FEBEX THM experiment using a state surface approach. International Journal of Rock Mechanics and Mining Sciences 42, 639–651.

Pahl, A., Heusermann, S., Bräuer, V., Glöggler, W., 1989. Grimsel Test Site. Rock Stress Investigations. Tech. rep., NAGRA Technical Report, 88-39E, Baden, Switzerland.

Rabung, T., Molinero, J., Garcia, D., Montoya, V., 2012. 1st Workshop Proceedings of the Collaborative Project Crystalline Rock Retention Processses, (7th EC FP CP CROCK). KIT Scientific Publishing, Barcelona, Spain.

Redfern, S. A., Angel, R. J., 1999. High-pressure behaviour and equation of state of calcite, CaCO3. Contributions to Mineralogy and Petrology 134 (1), 102–106.

Reuss, A., 1929. Berechnung der Fliegrenze von Mischkristallen auf Grund der Plastizitätsbedingung für Einkristalle. Journal of Applied Mathematics and Mechanics 9, 4958.

Rice, J. R., Cleary, M. P., 1976. Some basic stress diffusion solutions for fluidsaturated elastic porous media with compressible constituents. Reviews of Geophysics and Space Physics 14 (2), 227–241.

Rutqvist, J., Rejeb, A., M., T., Tsang, C.-F., 2003. Analyses of coupled hydrological-mechanical effects during drilling of the FEBEX tunnel at Grimsel. In O. Stephansson, J.A. Hudson and L. Jing (Eds), Proceedings of GeoProc 2003 (Stockholm, 196 13-15.10.2003) 44, 114–119.

Schaltegger, U., 1990a. Post-magmatic resetting of Rb-Sr whole rock ages - a study in the Central Aar Granite (Central Alps, Switzerland). Geologische Rundschau 79, 709–724.

Schaltegger, U., 1990b. The Central Aar Granite: highly differentiated calc-alkaline magmatism in the Aar Massif (Central Alps, Switzerland). European Journal of Mineralogy 2, 254–259.

Schaltegger, U., Corfu, F., 1992. The age and source of late Hercynian magmatization in the central Alps: evidence from precise U-Pb ages and initial Hf isotopes. Contributions to Mineralogy and Petrology 111, 329–344.

Schaltegger, U., Krähenbühl, U., 1990. Heavy rare earth element enrichment in granites of the Aar Massif (Central Alps, Switzerland). Chemical Geology 89, 49–63.

Schild, M., Siegesmund, S., Vollbrecht, A., Mazurek, M., 2001. Characterization of granite matrix porosity and pore-space geometry by in situ and laboratory methods. Geophysical Journal International 146, 111–125.

Schilling, F. R., Sinogeikin, S. V., Hauser, M., Bass, J. D., 2003. Elastic properties of model basaltic melt compositions at high temperatures. Journal of Geophysical Research: Solid Earth 108 (B6), 2304.

Selvadurai, A. P. S., 1996. Mechanics of Poroelastic Media. Kluwer Academic Publishers, The Netherlands.

Selvadurai, A. P. S., 2000. Partial Differential Equations in Mechanics. Vol. 2. The Bi-harmonic Equation, Poisson's equation. Springer-Verlag, Berlin.

Selvadurai, A. P. S., 2004. Stationary damage modelling of poroelastic contact. International Journal of Solids and Structures 41 (8), 2043–2064.
Selvadurai, A. P. S., 2007. The Analytical Method in Geomechanics. Applied Mechanics Reviews 60 (3), 87–106.
Selvadurai, A. P. S., 2009. Influence of residual hydraulic gradients on decay curves for one-dimensional hydraulic pulse tests. Geophysical Journal International 177 (3), 1357–1365.
Selvadurai, A. P. S., 2019. The Biot coefficient for a low permeability heterogeneous limestone. Continuum Mechanics and Thermodynamics 31, 939–953.
Selvadurai, A. P. S., Carnaffan, P., 1997. A transient pressure pulse method for the mesurement of permeability of a cement grout. Canadian Journal of Civil Engineering 24 (3), 489–502.
Selvadurai, A. P. S., Glowacki, A., 2008. Evolution of permeability hysteresis of Indiana Limestone during isotropic compression. Ground Water 46, 113–119.
Selvadurai, A. P. S., Głowacki, A., 2017. Stress-Induced Permeability Alterations in an Argillaceous Limestone. Rock Mechanics and Rock Engineering 50 (5), 1079–1096.
Selvadurai, A. P. S., Głowacki, A., 2018. Estimates for the local permeability of the Cobourg limestone. Journal of Rock Mechanics and Geotechnical Engineering 10 (6), 1009–1019.
Selvadurai, A. P. S., Letendre, A., Hekimi, B., 2011. Axial flow hydraulic pulse testing of an argillaceous limestone. Environmental Earth Sciences 64 (8), 2047–2058.
Selvadurai, A. P. S., Najari, M., 2015. Laboratory-scale hydraulic pulse testing: influence of air fraction in cavity on estimation of permeability. Géotechnique 65 (2), 126–134.
Selvadurai, A. P. S., Selvadurai, P. A., 2010. Surface permeability tests: Experiments and modelling for estimating effective permeability. Proceedings of the Royal Society A: Mathematical, Physical and Engineering Sciences 466 (2122), 2819–2846.
Selvadurai, A. P. S., Shirazi, A., 2004. Mandel-Cryer effects in fluid inclusions in damage-susceptible poroelastic geologic media. Computers and Geotechnics 31 (4), 285–300.
Selvadurai, A. P. S., Shirazi, A., 2005. An elliptical disc anchor in a damage-susceptible poroelastic medium. International Journal for Numerical Methods in Engineering 63 (14), 2017–2039.
Selvadurai, A. P. S., Suvorov, A. P., 2012. Boundary heating of poro-elastic and poro-elasto-plastic spheres. Proceedings of the Royal Society A: Mathematical, Physical and Engineering Sciences 468 (2145), 2779–2806.
Selvadurai, A. P. S., Suvorov, A. P., 2014. Thermo-poromechanics of afluid-filled cavity in a fluid-saturated geomaterial. Proceedings of the Physical Society A 470, 20130634.
Selvadurai, A. P. S., Suvorov, A. P., 2016. Thermo-poroelasticity and Geomechanics. Cambridge University Press, Cambridge.
Selvadurai, A. P. S., Suvorov, A. P., Selvadurai, P. A., 2015. Thermo-hydro-mechanical processes in fractured rock formations during a glacial advance. Geoscientific Model Development 8 (7), 2167–2185.
Selvadurai, P. A., Selvadurai, A. P. S., 2014. On the effective permeability of a heterogeneous porous medium: The role of the geometric mean. Philosophical Magazine 94 (20), 2318–2338.
Sisodia, P., Verma, M. P., 1990. Polycrystalline elastic moduli of some hexagonal and tetragonal materials. Physica Status Solidi 122, 525–534.
Stalder, H. A., 1964. Petrographische und mineralogiche Untersuchungen im Grimselgebeit. Schweizerische Mineralogische und Petrographische Mitteilungen 44, 187–398.
Steck, A., 1968. Die alpidischen Strukturen in den Zentralen Aaregraniten des westlichen Aarmassivs. Eclogae Geologicae Helvetiae 61, 19–48.
Suvorov, A. P., Selvadurai, A. P. S., 2011. Effective medium methods and a computational approach for estimating geomaterial properties of porous materials with randomly oriented ellipsoidal pores. Computers and Geotechnics 38, 721–730.
Suvorov, A. P., Selvadurai, A. P. S., 2019. The Biot coefficient for an elasto-plastic material. International Journal of Engineering Science, In press.
Talbot, D. R., Willis, J. R., Nesi, V., 1995. On improving the Hashin-Shtrikman bounds for the effective properties of three-phase composite media. IMA Journal of Applied Mathematics (Institute of Mathematics and Its Applications) 54 (1), 97–107.
Terzaghi, K., 1923. Die Berechnung der Durchlassigkeitsziffer des Tones aus Dem Verlauf der Hydrodynamischen Spannungserscheinungen, Akad. Wissensch. Wien Sitzungsber Mathnaturwissensch Klasse IIa 142, 125–138.
Ting, T. C. T., 1996. Anisotropic Elasticity: Theory and Applications. Oxford University Press, Oxford.
Verruijt, A., 2015. Theory and Problems of Poroelasticity. Delft University of Technology, The Netherlands.
Voigt, W., 1928. Lehrbuch der Kristallphysik, B.G. Teubner. Leipzig.
Walpole, L., 1966. On bounds for the overall elastic moduli of inhomogeneous systems–I. Journal of the Mechanics and Physics of Solids 14, 151–162.
Wang, H. F., 2000. Theory of Linear Poroelasticity with Applications to Geomechanics and Hydrogeology. Princeton University Press, Princeton.
Wenning, Q. C., Madonna, C., de Haller, A., Burg, J. P., 2018. Permeability and seismic velocity anisotropy across a ductilebrittle fault zone in crystalline rock. Solid Earth 9, 683–698.

Wüthrich, H., 1965. Rb-Sr-Altcrsbestimmungen am alpin berprgten Aarmassiv. Schweizerische Mineralogische und Petrographische Mitteilungen 45, 876–971.

Yue, Z. Q., Selvadurai, A. P. S., 1995. On the mechanics of a rigid disc inclusion embedded in a fluid saturated poroelastic medium. International Journal of Engineering Science 33 (11), 1633–1662.

Zhu, W., Hughes, J. J., Bicanic, N., Pearce, C. J., 2007. Nanoindentation mapping of mechanical properties of cement paste and natural rocks. Materials Characterization 58, 1189–1198.

Ziegler, M., Amann, F., 2012. Laboratory test results obtained from core samples from the Grimsel III borehole at Kessiturm. Tech. rep., Internal Report, Ingenieurgeologie, ETH Zurich.

Zimmerman, R. W., 1991. Compressibility of Sandstones. Developments in Petroleum Science, Elsevier, Amsterdam.